

Theoretical study for estimation of the dynamic stress intensity factor from results of an experimental measurement

Matúš Turis^{1,*}, *Milan Držík*² and *Ol'ga Ivánková*¹

¹Slovak University of Technology in Bratislava, Faculty of Civil Engineering, Radlinského 11, 810 05 Bratislava, Slovak Republic

²International Laser Center, 841 04 Bratislava, Slovak Republic

Abstract. The aim of this contribution is a theoretical study for the estimation of the dynamic stress intensity factor (DSIF) using results from an experimental measurement. Using optical methods, it is possible to determine individual displacements of crack surfaces in multiple distances from the crack tip. Based on the theoretical distribution of displacements in the crack front, the DSIF can be estimated using the displacement extrapolation method at each time step. The main motivation for this methodology is the difficulty of estimation DSIF in real structures. The described approach is consequently compared with conventional numerical methods and the applicability is evaluated.

1 Introduction

There are several methods for determining the DSIF. The first group of methods can be called numerical ones. In this group, DSIF is calculated based on results from numerical analysis. Numerical methods for estimation DSIF are for example interaction integral method [1], direct calculation from distribution of stresses and displacements around the crack tip [2], concurrent multigrid method [3], material point method from the dynamic stress solution [4], etc. There are also hybrid methods that combine experimental measurements from which the results are compared and used in numerical analysis to determine the DSIF. Measured applied loads and fracture time have been used in the numerical analysis to determine fracture toughness in [5]. As inputs to numerical analysis experimentally measured forces and velocities were taken to compute crack opening displacement and responsible DSIF in [6]. The third group of methods is directly estimated DSIF from an experimental measurement. Measured change of SIF at fatigue crack with digital image correlation using decomposition of displacement field onto a tailored set is presented in [7]. The submitted contribution deals with the estimation of DSIF directly from experimental measurement by the displacement extrapolation method. This approach is chosen due to the difficulty of capturing the boundary conditions of a cracked body in

* Corresponding author: matus.turis@stuba.sk

real structures. From our initial experimental measurement, we found out that relatively small changes in placement of the cracked body highly affect measured results.

2 Description of problem

Selected geometry of single edge notch specimen (SEN) and impulse load are shown in Fig. 1. Signs of specimen dimensions are as follows: $2L$ -length; W -width; B -thickness; a -crack length. The specimen is unbonded and loaded by impulse force in the form of a half-wave sine. Impulse force duration equals to twelfth of the crack opening period. The position of force is in the middle between the crack and free end in a longitudinal direction. The length of crack equals to half of the specimen width.

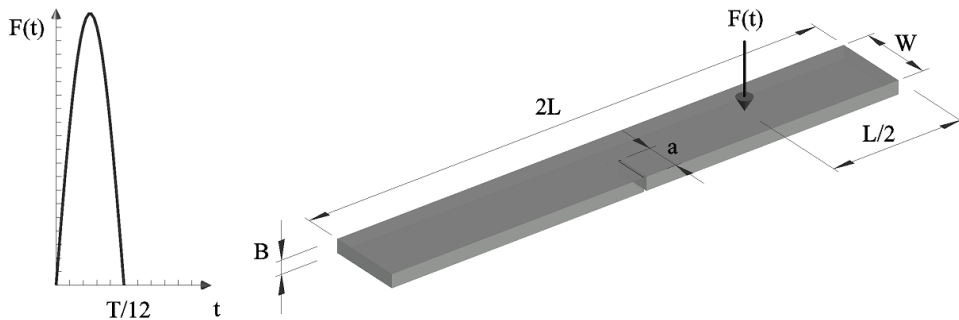


Fig. 1. Selected geometry (SEN) and impulse load.

The task is to determine DSIFs directly from measured displacements in time and three coordinate axis x , y , z . Such a measurement can be performed using optical methods.

3 Methodology

The assumptions of calculation are experimentally or numerically achieved displacements in multiple positions ahead of the crack tip. In this paper, the displacements were obtained from finite element analysis. From these displacements, DSIFs were calculated using the displacement extrapolation method (DEM). Reference values of DSIFs were set to be the results of the interaction integral method [8]. Results of DSIFs that were obtained by DEM can be considered as independent with respect to those obtained by interaction integral method. In our case, the calculated displacements can be considered as experimentally measured, for subsequent comparison.

Only displacements on the free faces of the specimen can be measured experimentally. Based on finite element analysis DSIFs are known at a lot of through body thickness position. Due to this fact it is possible to compare the results of both methods at multiple through body thickness position. Chosen positions are at the side where the force acts (F-side), on the opposite side (O-side) and in the middle of body thickness.

4 Basic assumptions of calculation

The crack can be loaded in three different modes. The product of each mode is the motion of crack faces in one of three local coordinate axes. The planar view and definition of the local coordinate system of crack are shown in Fig. 2. According to Fig. 2, mode I causes opening deformation Δv in y coordinate. Mode II produces in-plane shear deformation Δu

in x coordinate and mode III out of plane shear deformation Δw in z coordinate. In the case of linear elastic fracture mechanics, the solution of a general case can be described by a superposition of these three base modes [9].

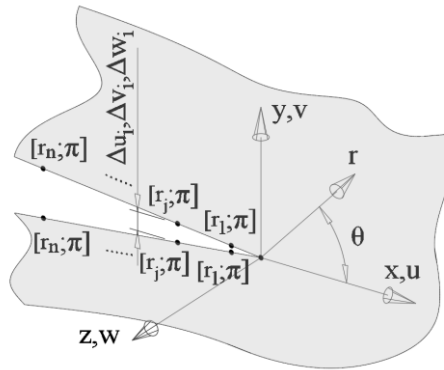


Fig. 2. Planar view of crack with the definition of the local coordinate system of crack, polar coordinates, and points needed for DEM.

One stress intensity factor (SIF) belongs to one mode. With known SIF it is possible to estimate stress and displacement fields in the crack tip vicinity. From measured or computed displacement field it is possible to calculate individual SIF or DSIF. Theoretical distribution of displacements ahead of a crack tip ($\theta = \pi$) leads to equations

$$\begin{aligned}
 K_I(t) &= \lim_{r \rightarrow 0} \left[\frac{E \Delta v(t)}{8 - 8\nu^2} \sqrt{\frac{2\pi}{r}} \right] \\
 K_{II}(t) &= \lim_{r \rightarrow 0} \left[\frac{E \Delta u(t)}{8 - 8\nu^2} \sqrt{\frac{2\pi}{r}} \right] \\
 K_{III}(t) &= \lim_{r \rightarrow 0} \left[\frac{E \Delta w(t)}{8(1+\nu)} \sqrt{\frac{2\pi}{r}} \right]
 \end{aligned} \tag{1}$$

where $K_i(t)$ are individual DSIFs ($i = I, II, III$), E is the Young modulus, ν is the Poisson ratio and the rest is obvious from Fig. 2. Note that the plane strain conditions are considered due to the expectation of high-stress concentration in the crack tip vicinity.

Equations (1) contains a singular term $1/\sqrt{r}$. To solve individual DSIF it is needed to achieve three-dimensional function $K_i^h(r, t)$, which is the result of individual equation (1) with respect to polar coordinates r and time t . At each time this function has a rising or falling tendency with respect to r . This tendency is according to the sign of individual movement of crack faces. Resulting K_i is then the projection of this function into the plane for $r = 0$. This problem can be solved using a linear trendline [10]. In this case, the general equation is as follows

$$T(r) = kr + K_i \tag{2}$$

where $T(r)$ is a trendline with respect to r and k, K_i are constants. Because the trendline must be calculated at each considered time separately, K_i in this equation is not with respect to time.

The equation to compute k for general $K_i^h(r_j)$ is

$$k = \frac{n \sum r_j K_{ij}^h - \sum r_j \sum K_{ij}^h}{n \sum r_j^2 - (\sum r_j)^2} \tag{3}$$

where n is a count of considered distances r_j from the crack tip, $j = 1 \dots n$, K_{ij}^h is calculated from equation (1) for given i -th mode at distance r_j .

Finally, the equation for estimation K_i is

$$K_i = \frac{\sum K_{ij}^h - k \sum r_j}{n} \tag{4}$$

All summation signs in equation (3, 4) are for $j = 1 \dots n$. After the solution for every considered time is done, the results of $K_i(t)$ are known.

5 Results and discussion

Shown results are the comparison of two methods for estimation DSIF. As reference values were set those achieved by interaction integral method and compared to the method described above. Resulting time records of K_I and K_{II} on the F-side are shown in Fig. 3.

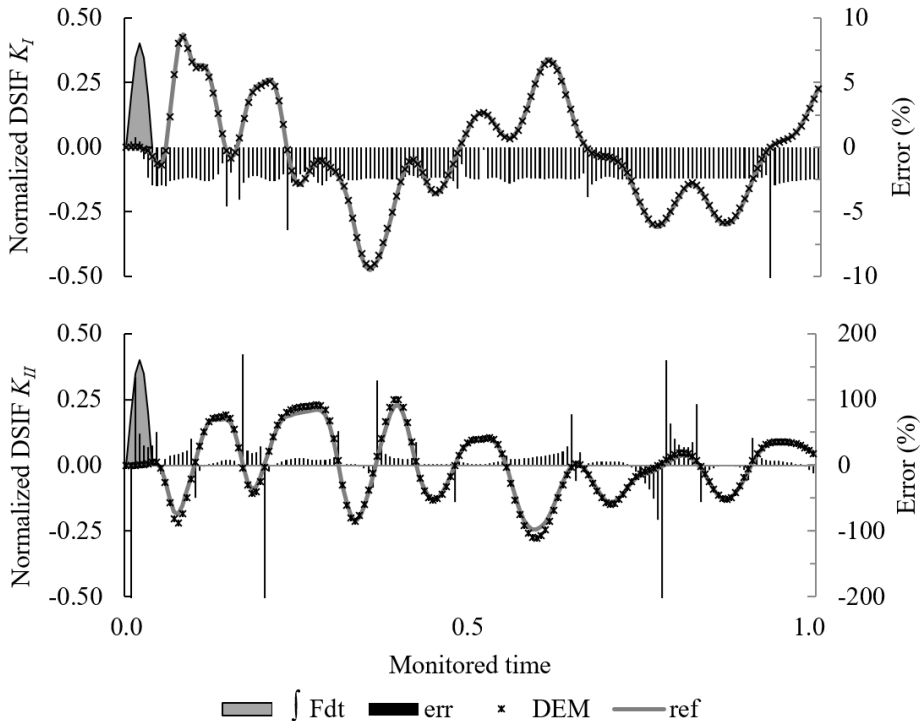


Fig. 3. Comparison of normalized DSIFs on F-side of the specimen obtained by two methods and time record of solution error.

Individual DSIFs in Fig. 3 are normalized by static stress intensity factor on SENT (single edge notch tension specimen) that is loaded by force equal to the amplitude of impulse force. Time records of K_I and K_{II} on the O-side are mirror images of F-side through the time axis. At the body thickness middle point, mode I and II reached negligible values. Results

of $K_{III}(t)$ at the monitored time has almost the same value through the entire body thickness. The shape and values of $K_{III}(t)$ are similar to those achieved for $K_{II}(t)$ on F-side.

It can be seen that maximum errors in results are at times where DSIFs are crossing the zero values. For further statistical evaluation, these errors were removed. Graphically presented results of errors are in Fig. 4.

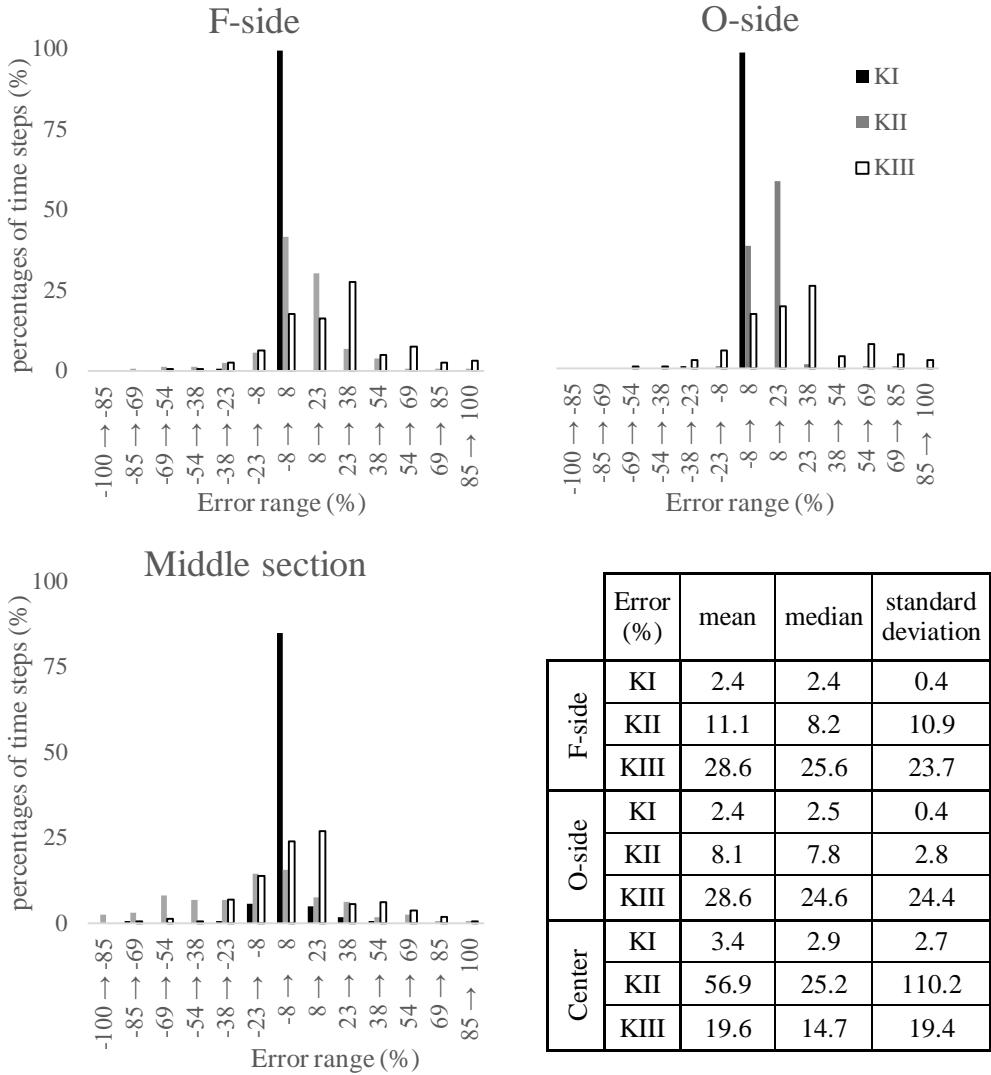


Fig. 4. Percentages of considered time steps that satisfy the error range between results. Selected statistical indicators.

Errors were calculated also as absolute values and considering the signs. To obtain selected statistical indicators absolute values of errors were used. For the determination of higher or lower values than the reference ones, the errors with the sign were used. After removing the extreme errors, at a time when DSIF crosses zero value, there remained still 95% of the time steps to consider. Results showed in Fig. 4 and the attached table are from this data set.

Almost an ideal correlation of values was reached for $K_I(t)$. Also, $K_{II}(t)$ has reached a good agreement of values. The lowest match was found to be $K_{III}(t)$ values at the free faces

of the specimen. It can be affected by the fact that the three-dimensional interaction integral corresponds to a weighted average over a finite crack-front length. It means that theoretically interaction integral value on the free surface is zero [9]. Due to mentioned, $K_I(t)$ was not taken strictly from the free surface but two elements away. Calculation points for DEM were taken at the same position. It helped for $K_I(t)$ and $K_{II}(t)$ values although the peak of percentage errors of $K_{II}(t)$ is slightly shifted to the right. At the midpoint of body thickness, only one non-negligible value was $K_{III}(t)$ with a satisfying correlation to the reference value.

6 Conclusion

The aim of this contribution was to assess the usability of the displacement extrapolation method for the estimation of dynamic or static stress intensity factor. It is being planned to use this approach in experimental measurements. In this paper, a comparison of two methods for determining this parameter is presented. Used methods are based on different principles. The interaction integral method is a very complex one for estimation SIF or DSIF that can deal with various crack geometries and is more or less mesh independent. On the other hand, it can be used only in numerical analysis. It is often a very difficult task to fit the right boundary conditions of real structure in numerical analysis. Especially in the case of a dynamically loaded body, relatively small changes in describing the interaction of two or more parts affect obtained results considerably. The displacement extrapolation method presented in this paper is a simple method with a lot of limits regarding crack geometries. But it is an effective tool for cases like the above-presented one and can be used in the experimental measurement of simple crack geometries. The effectiveness of this method lies in the relative simplicity of obtaining inputs. Measuring the movements of multiple pairs of points ahead of the crack tip can be done in different ways. By evaluation of the camera record when the crack face motion frequency is enough times smaller than the camera sampling rate, or for higher frequencies of crack face movements, by capturing the passing light through a pre-formed slit, etc.

This article was written thanks to the grant program SK-VEGA 1/0412/18 and SK-KEGA 025 STU-4/2019.

References

1. S. Song, G. Paulino, *Int. J. Solids and Struct.* **43** (2006)
2. X. Tian, Ch. Du, S. Dai, D. Chen, *Struct. Eng. Mech.* **66** (2018).
3. J. Ch. Passieux, A. Gravouil, J. Réthoré, M. Ch. Baietto, *Int. J. for Num. Met. in Eng.*, **85**, 1648 – 1666 (2011)
4. Y. GUO, J. Nairn, *Comp. Mod. in Eng. Sc.*, **16** (2006)
5. G. Weisbrod, D. Rittel, *Int. J. of Frac.*, **104** (2000)
6. H.D. Bui, H. Maigre, D. Rittel, *Int. J. Solids and Struct.* **29**, 2881-2895 (1992)
7. R. Hamam, F. Hild, S. Roux, *Strain*, **43**, 181 – 192 (2007)
8. ANSYS® Academic Research Mechanical, Release 17.2, Help System, Coupled Field Analysis Guide, ANSYS, Inc.
9. T.L. Anderson, *Fracture mechanics Fundamentals and Applications*, 688 p. (1995)
10. S. Puntanen, *Int. Statist. Rev.*, **78**, 144-144 (2010)